Arch. Metall. Mater. **66** (2021), 2, 461-468

DOI: 10.24425/amm.2021.135879

FIROUZEH MOTAMAD DEZFULI[1], ARASH BOOCHANI[2*],
SARA SADAT PARHIZGAR[1], ELHAM DARABI[1]

THE Ru IMPURITY EFFECT ON ELECTRONIC, OPTICAL AND THERMOELECTRIC PROPERTIES OF MoS_2 NANO-SHEET: A DFT STUDY

The electronic, optical and thermoelectric properties of MoS_2 nano-sheet in presence of the Ru impurity have been calculated by density functional theory framework with Generalized Gradient approximation. The $MoRuS_2$ nano-sheet electronic structure was changed to the n-type semiconductor by 1.3 eV energy gap. The optical coefficients were shown that the loosing optical energy occurred in the higher ultraviolet region, so this compound is a promising candidate for optical sensing in the infrared and visible range. The thermoelectric behaviors were implied to the good merit parameter in the 100K range and room temperatures and also has high amount of power factor in 600K which made it for power generators applications.

Keywords: MoS_2Ru nano-sheet, DFT, Electronic properties, Optical properties, Thermoelectric Properties

1. Introduction

The physical properties of two-dimension (2D) materials have been opened the new windows in the material sciences [1-4]. Transition-metal dichalcogenides (TMDs), have been more attractive due to their electronic, optical and thermoelectric properties, which are originated in the quantum effects by the atomic-layer of TMD crystals. The two-dimensional (2D) transitions metals as MoX_2 (X = S, Se and Te) have been attractive for science and industry based on their electronic, mechanical, thermoelectric, sensors and photo-detectors properties [5-7] as a surrogate for silicon or organic semiconductors. The MoX_2 2D structures have a Mo layer which is sandwiched with two X layers. Several physical properties of MoX_2 have been investigated in the bulk, film and 2D forms, experimentally and theoretically [8-11]. The MoS_2 nano-sheet is synthesized by mechanical exfoliation technique [12], liquid exfoliation [13] and chemical vapor deposition (CVD) [14,15], physical vapor deposition (PVD) [16] etc.

The experimental efforts were reported that the MoS_2 bulk has an indirect band gap by 1.29 eV, meanwhile, its monolayer with 0.65 nm thickness has the 1.8 eV p-type direct gap [17], which is referred to contribute to low-power electronics, thermoelectric and flexible optoelectronic applications [18-21]. Moreover, this compound is used for energy conversion [22], energy storage [23], and hydrogen evolution [24]. The electronic and optical properties of MoS_2 2D are depended on the same conditions as thickness, defects and impurities, and then need to be understood in detail for the suitable design of devices and their functions [8].

The photoresponsivity of MoS_2 mono-layer was reported as 880 $A.W^{-1}$ for incident light at a wavelength of 561 nm with photoresponse in the 400-680 nm range [25], which can be applied in the ultra-sensitive phototransistors. The photoluminescence and absorption capacity of MoS_2 mono-layer [26] in the ultraviolet area, makes it a promising composition for the ultraviolet detectors [27] and absorber layer in low-cost film solar cells [28-29] and light-emitting diodes (LEDs) [30-34].

Some works have investigated the thermoelectric behaviors of MoS_2 nano-sheet [35-39] to solve energy issues. The efficiency of thermoelectric material is shown by the figure of merit (ZT), which is related to the Seebeck (S), electronic conductivity (σ) and thermal conductivity (K). The ZT of MoS_2 2D lies between 0.02 to 0.53 [40], and some experiment efforts have been shown that this composition is a good thermoelectric material with a large S parameter [41]. Some studies have been shown the effect of the vacancy, defects and doping impurities on the thermoelectric efficiency of MoS_2 2D. The good thermoelectric

[1] DEPARTMENT OF PHYSICS, FACULTY OF SCIENCES, SCIENCE AND RESEARCH BRANCH, ISLAMIC AZAD UNIVERSITY, TEHRAN, IRAN
[2] DEPARTMENT OF PHYSICS, KERMANSHAH BRANCH, ISLAMIC AZAD UNIVERSITY, KERMANSHAH, IRAN

* Corresponding author: arash_bch@yahoo.com

material must behave the ZT near one or greater than one amount, so investigating for new forms of MoS_2 nano-sheets by adding the impurities of vacancies seems to be necessary.

A recent study has been reported that the MoS_2 mono-layer has high thermopower [42], also, other work was indicated a high ZT amount of 1.6 this case [43]. The strain effect on the MoS_2 was investigated by Bhattacharyya et al. [44]. Achieve higher thermal conductivity and the ZT parameter is still the greatest challenge in material science. Jin et al. [45] calculated the high thermal conductivity of single-layer MoS_2, i.e.116.8 $Wm^{-1}K^{-1}$ resulting in a relative low ZT value of 0.26 at 500K. Increasing the electrical conductivity and decreasing the thermal conductivity of MoS_2 is essential for its thermoelectric applications. In this paper, we added the Ru impurity to the MoS_2 nano-sheet and investigated the electronic, optical and thermoelectric properties of the $MoRuS_2$ nano-sheet.

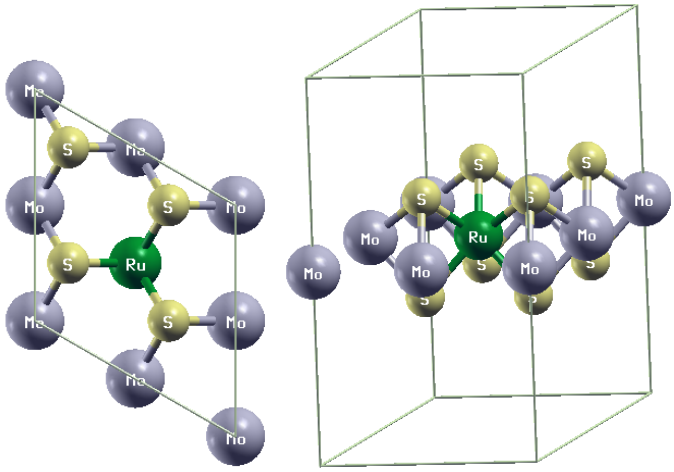

Fig. 1. The crystal shape of the $MoRuS_2$ nano-sheet

2. Calculations method

The calculations were carried out by the WIEN2K code based on the density functional theory (DFT), using the full-potential linear augmented plane wave (FP-FLAPW) method and GGA approximation for the determination of exchange-correlation potential [46-48]. The optimized input parameters for calculations are RKmax = 8.5, lmax = 10, Gmax = 13.5, and RMT = 2. Also, the KPoint for the pure and impurity cases are selected to 1000 and 500, respectively, by Mankhorest pack model [49]. All atoms' positions are relaxed using the mini-position program, the convergence of force is selected to be 0.1 mRyd/a.u. The optical calculations have been approximated by random phase approximation (RPA) [50]. The thermoelectric calculations were done by BoltzTraP code [51], which its input parameters are used of the Wien2K outputs. Fig. 1 is shown the MoS_2 and $MoRuS_2$ graphene crystals which are depicted by XCrysden software.

3. Results

3.1. Electronic properties

The electronic structure of the materials such as bandstructure and density of states (DOS) contains important information about electronic, optical and thermoelectric properties. The bandstructure diagrams of the MoS_2 graphene and in the presence of the Ru impurity along the symmetry direction of their first Brillouin zone have been shown in Fig. 2. The MoS_2 pure is the p-type semiconductor by a direct energy gap at K point with 1.8 eV amount which is in agreement with other reported. Based on the p-type character for this case, the MoS_2 graphene can be a candidate for thermoelectric applications. The low density of the levels around the Fermi level reduces the thermoelectric efficiency, as mentioned in other works "0.02 to 0.53 range" [40]. The MoS_2 electronic structure by this energy gap indicated that this material attractive in optoelectronic devices [18-21]. The Ru element by [Kr] $4d^7 5s^1$ orbitals shape is a transition metal with

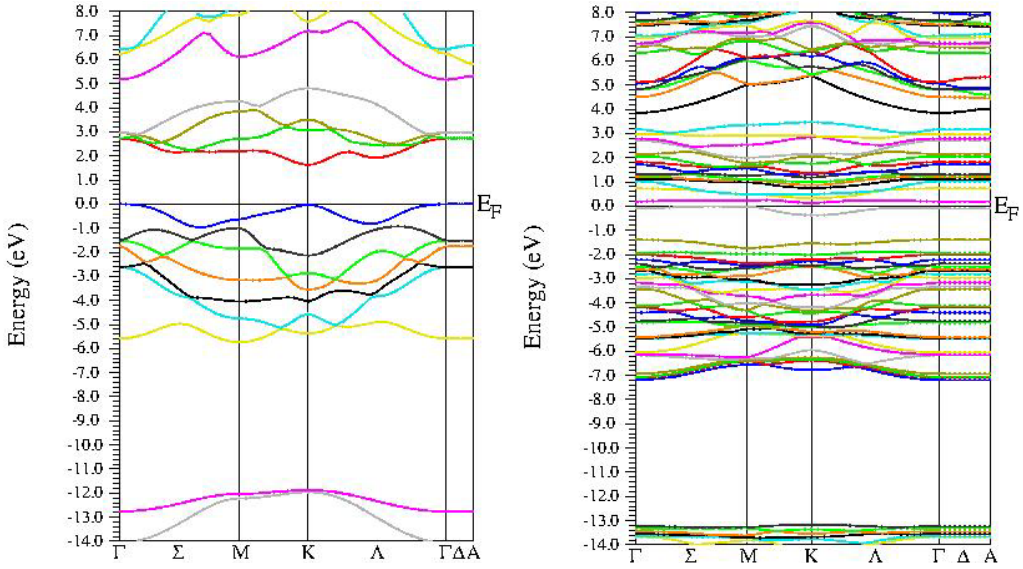

Fig. 2. The Bandstruture of MoS_2 (left) and $MoRuS_2$ (right) nano-sheets versus the symmetry directions of first Brillouin zone

high metal capability which can be an important role to change and control the electronic, optical and thermoelectric behavior. The $MoRuS_2$ bandstructure along the symmetry direction of the Brillouin zone has been shown in Fig. 2(b), which refers to the semiconductor behavior. Except around the K point, in the other symmetry points the level which cut the Fermi level slop is zero, so the electron mobility is very high and this composition is the n-type semi-metallic with 1.3 eV gap. Increasing the density of levels in the valance band maximum (VBM) and conduction band minimum (CBM) can make a thermoelectric compound of $MoRuS_2$ graphene. Add the Ru to MoS_2 graphene has been shifted the levels and the energy gap toward the lower energies.

The DOS diagrams of the MoS_2 and $MoRuS_2$ nano-sheets have been considered in Figs. 3 and 4 which are in agreement with the bandstructure diagrams. The total DOS of MoS_2 is shown the continued behavior in the valance and conduction ranges which are separated be a 1.6 eV gap, implying a good base for the excited electrons for transports. The DOS curve is tangent to the Fermi level but and the van-hove singularities are exists in the VBM and CBM. The Mo-d and S-p overlapping under the Fermi level is referred to strong bonds between them. Add the Ru metal and replaced to the Mo site has been changed the electronic behavior in the $MoRuS_2$ (See Fig. 4). The Mo has [Kr] $4d^5 5s^1$ orbitals form and Ru has [Kr] $4d^7 5s^1$ the orbitals structures, so increasing the d orbital electrons have been caused to shift the density of states to the lower energies. The total DOS is shown the nonmagnetic behavior which for better comparison we zoom on the states in the Fermi range at Fig. 4(a). Also, the energy gap is shifted to under Fermi level while decreased it to 1.2 eV and the electron states on the Fermi are perpendicular to the energy axis which referred to the van-hove singularity. The main contributions of the electron states at the Fermi level belong to the Mo-, Ru-d and a few S-p Fig. 4(b-d). Increasing the states at the Fermi level will be effected by the optical and thermoelectric properties. Fig. 4 is shown that the maximum sates of electrons are originated of Ru-d orbitals. So, we expected to add Ru impurity to the MoS_2 graphene structure to modify the optical and thermoelectric behaviors. The Eu-d overlapping with the Mo-d and S-p orbitals has been generated the energy band gap in the –1.5 eV to –0.5 eV energy range. These orbitals make the electronic instability in the Fermi which referred to the van-hov singularity. Also, these orbitals have the main contribution to the conduction bands.

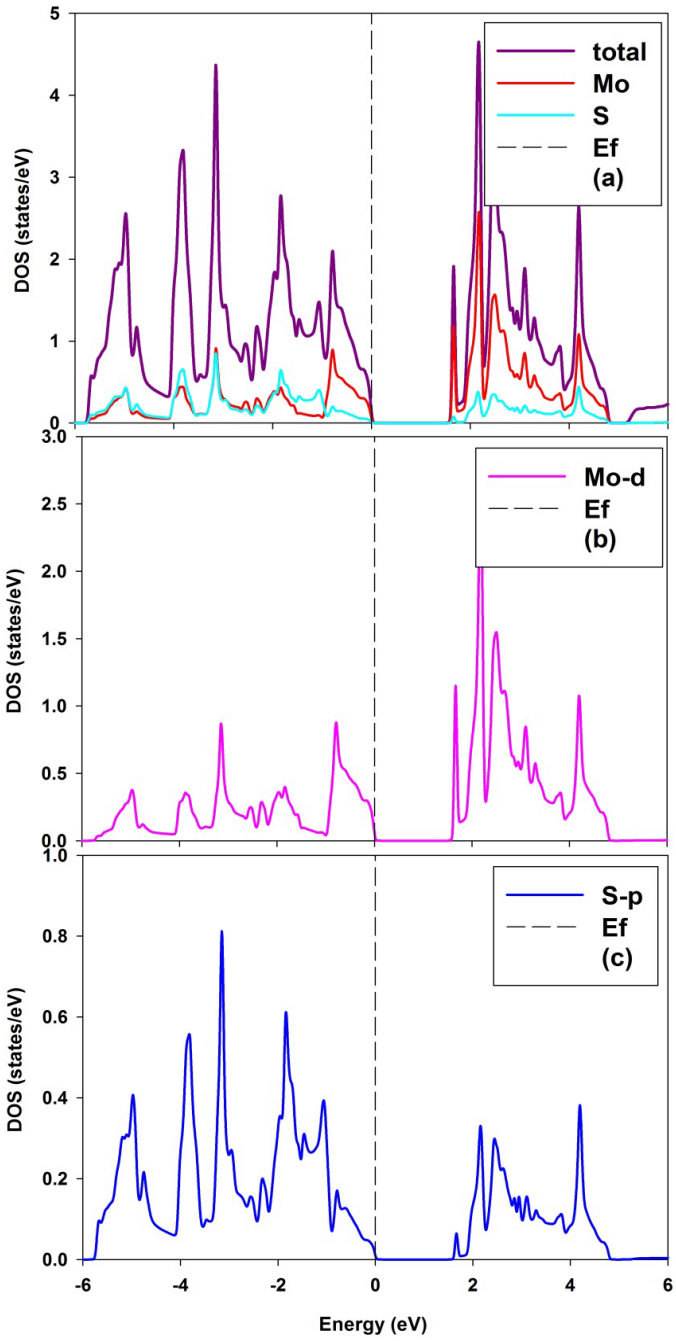

Fig. 3. The total and atomic DOS of the MoS_2 nano-sheet

3.2. Optical Properties

The dielectric function, $\varepsilon(\omega)$ is a complex tensor that describes the optical response of the matter to the light and serves as a source to extract other optical parameters based on the Kramers-Kronig relations [52,53]. The $\varepsilon(\omega)$ ontains two real ($Re\ \varepsilon(\omega)$) and imaginary ($Im\ \varepsilon(\omega)$) which indicated the optical response of the material in the real and imaginary spaces. The $Re\ \varepsilon(\omega)$ of the $MoRuS_2$ nano-sheet has been shown in the Fig. 5(a) for two perpendiculars (zz) and in-plane (xx) directions. The $Re\ \varepsilon(\omega)$ has the anisotropy behavior along with the two mentioned directions of zero to 5eV photon energy and after this energy has isotropic behavior. The static amount of the $Re\ \varepsilon(\omega)$ along *xx* has several times greater than *zz* one which referred to the semi-metallic nature along *xx* and semiconductor property along *zz* direction. But in the infrared region, it is shown the optical instability along *xx* because of the sharp dropping of the $Re\ \varepsilon(\omega)$ diagram and then has a peak at the visible area and has decreased to zero vicinity in 5eV. On the other hand along with the *zz* one it has more stability in the zero to 5eV interval and dropped in the end of this range. It is several $Re\ \varepsilon(\omega)$ roots in the ultra violet (UV) area and its amount is near the zero which. The $Im\ \varepsilon(\omega)$ curve peaks have been shown the optical transitions at the full orbitals to the empty

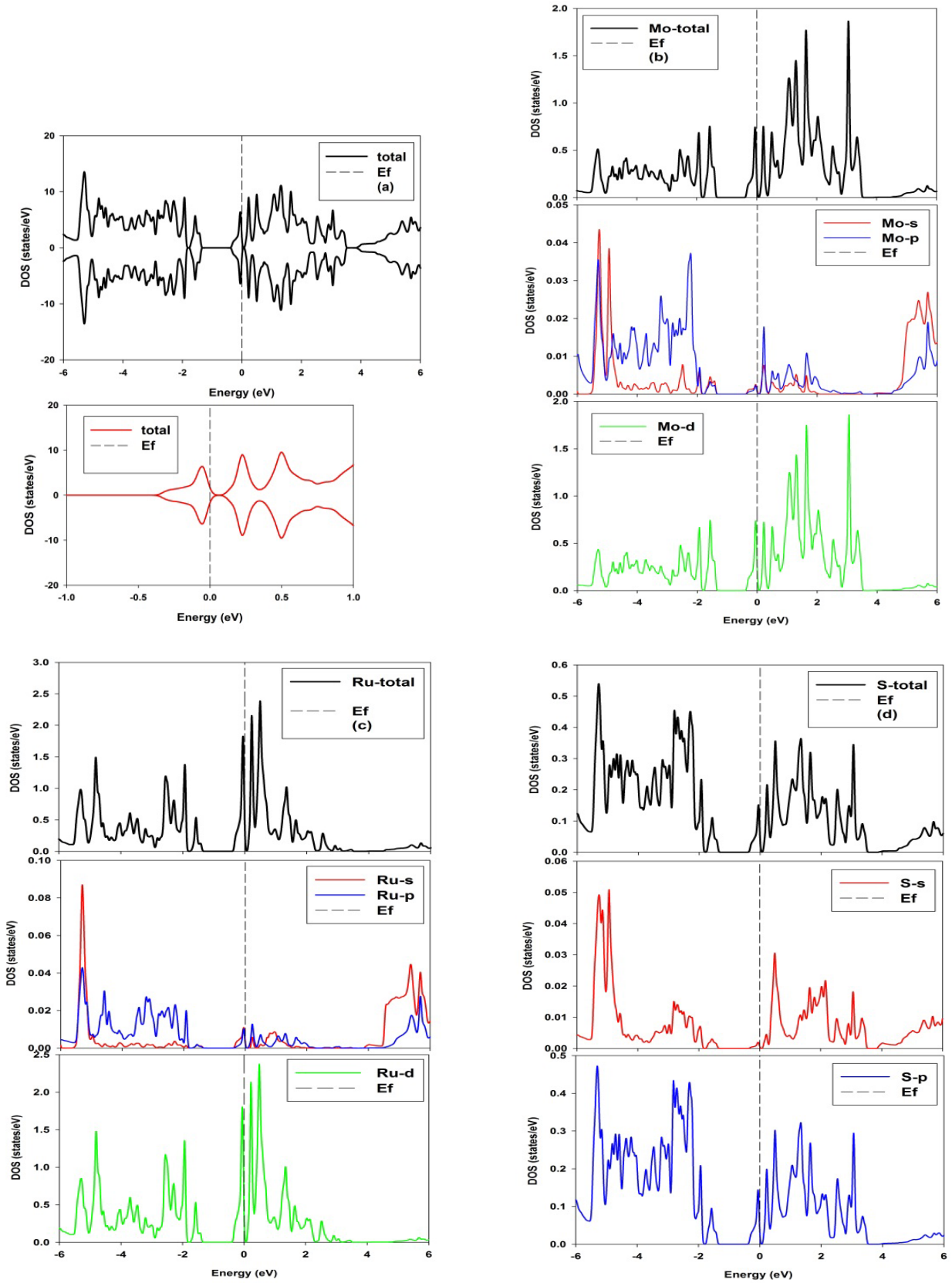

Fig. 4. The total and partial DOS of $MoRuS_2$ nano-sheet

ones. Fig. 5(b) is displayed the semi-metallic behavior along *xx* direction but has semiconducting treatment in the IR and the visible area of *zz* one. After the Dirac peak at 0.35eV, two little peaks are located in a visible area and one great peak is in the UV edge for *xx*, but the main peak of *zz* one has the blue-shifted which is located at 5eV. By increasing energy after 5eV, the *Im* e(w) diagrams are shifted to zero which referred to the vacuum nature along two mentioned directions. The energy loss function

(Eloss) is an important parameter to find the reasons of losing the photon energy (Fig. 5(c)). It is indicated that the Eloss great peaks of the two mentioned directions are in the 15eV to 20eV interval while the *Re* $\varepsilon(\omega)$ has the roots for *xx* and *zz* directions. So the plasmonic frequencies for the mentioned directions are occurred in higher photon energy and the $MoRuS_2$ graphene can be proposed for optical applications in the IR and visible area. The Eloss low amount and high amounts of the *Re*- and *Im* $\varepsilon(\omega)$ in the IR and along the *xx* direction indicated the very good optical absorption with low energy loss in this area.

The optical conductivity (Sigma), Absorption and Reflection of the $MoRuS_2$ nano-sheet have been depicted for *xx* and *zz* directions which have the anisotropy in the lower energies. It is shown that the optical conductivity at zero energy is very low for *xx* which referred to the semiconducting nature by zero gap and is fully semiconductor along with another direction (Fig. 6(a)). But the higher amounts of Sigma have occurred at 5 eV and 11 eV for *xx* direction. In the higher energies, the optical conductivity shifted to zero and also the Reflections of the two directions are very low which is referred to transparent nature of this compound. The Absorption along *zz* has a gap nearly to the electronic gap and has a very small gap along *xx* one which indicated semi-metal behavior in this direction. By increasing photon energy the absorption of the mentioned directions are increased dramatically in the visible and UV edge of *xx* and *zz* directions, respectively. Comparing the optical Reflections agree on the semi-metallic nature along *xx* because of its static amount and is very low in the *zz* one. The Reflections at high energies shifted to low amounts which originated from the transparent behavior of this compound.

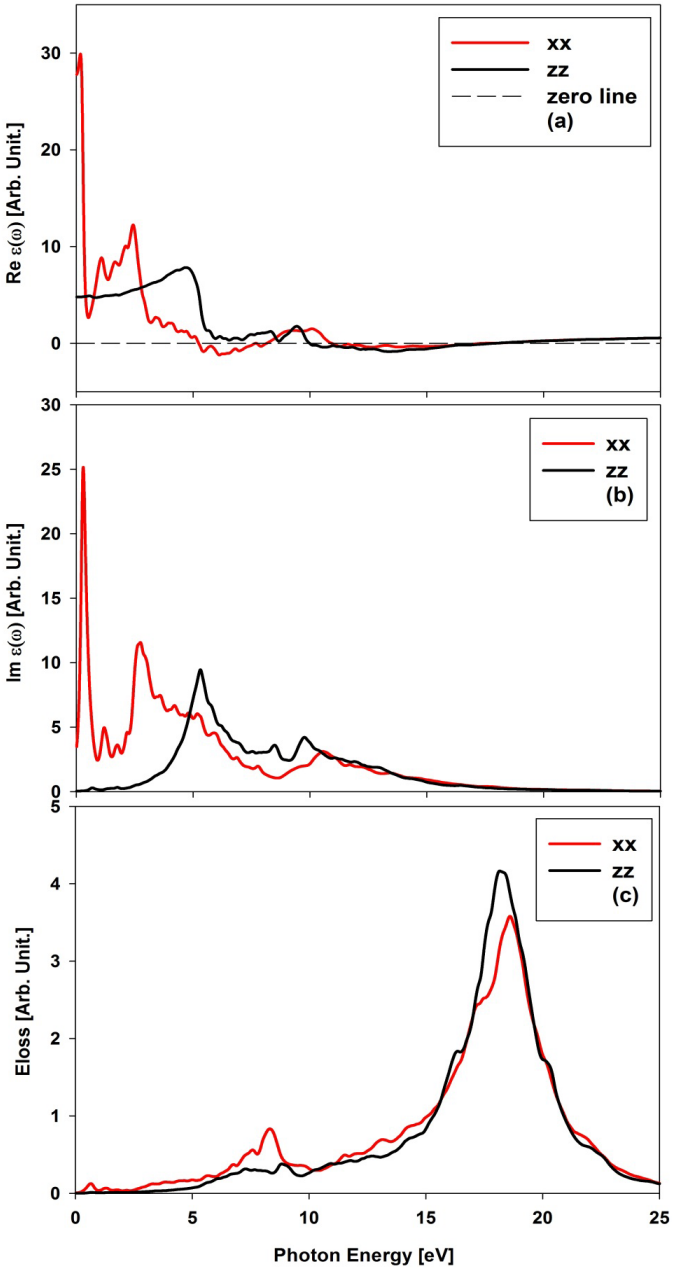

Fig. 5. The *Re-, Im* $\varepsilon(\omega)$ and Eloss versus photon energy in the (a-c) panels

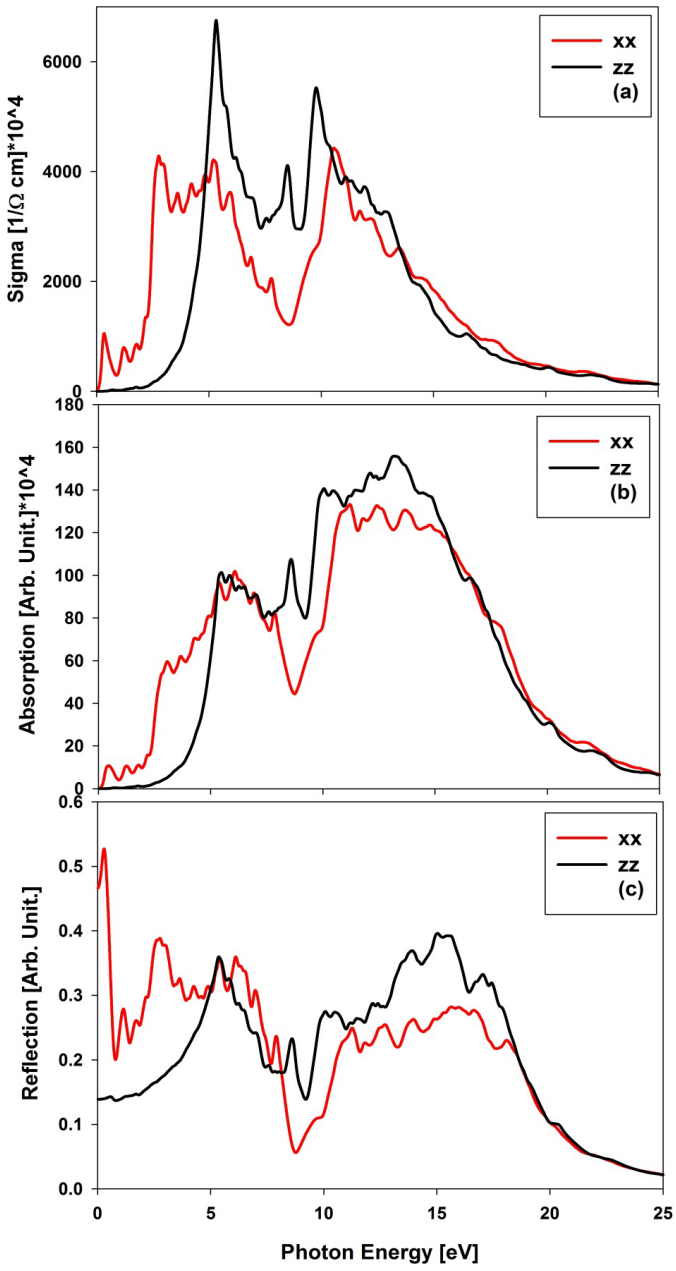

Fig. 6. (a) The optical conductivity (Sigma), (b) Reflection of the $MoRuS_2$ nano-sheet versus photon energy along the *xx* and *zz* directions

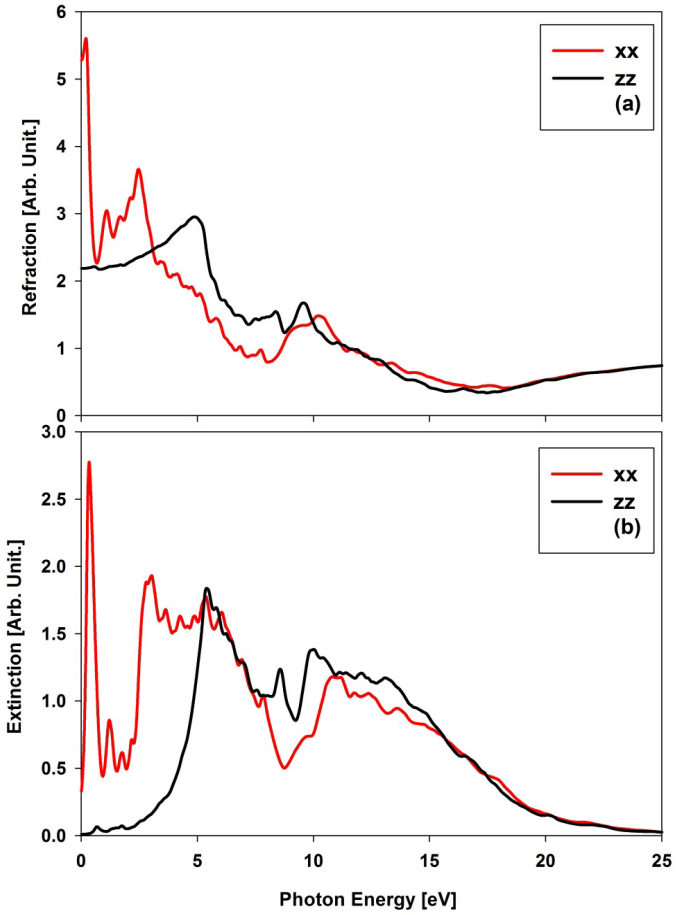

Fig. 7. (a) The Refraction and (b) Extinction of the $MoRuS_2$ nano-sheet along the sheet (*xx*) and perpendicular to it (*zz*)

3.3. Thermoelectric

The gradient temperature can be made the potential difference or, this process occurs inversely in thermoelectric materials. So these materials have an important position in the electronic and thermoelectric industry. Thermoelectric materials have attracted intense interest due to wide applications in chip cooling, power generation, and infrared sensing [54-56]. Within the framework of the constant scattering time approximation, the Seebeck (S), Power factor (P), merit coefficient (ZT), thermal (K) and electronic (s/t) conductivities of the $MoRuS_2$ nano-sheet have been depicted in Fig. 8. The good thermoelectric materials must have a narrow band gap and multiple bands near the band edges. The s/t diagram versus temperature is shown in Fig. 8(a) which is zero till 200K which is referred to the semiconductor nature and after this temperature is increased with a steep slope. The thermal conductivity has been displayed the same behavior of s/t in Fig. 8(b), but its amount in any temperature than other compound is a good sign for increase ZT. The S is a sensitive tool for knowing the electronic structure near the Fermi level. The S has a very low amount for metals (in order of mVK^{-1}) and much higher for semiconductors. The high value and positive sign of the S parameter for the $MoRuS_2$ in Fig. 8(d) has been confirmed the p-type concentration by good thermoelectric property. The high value from S is originated of the flat levels around the gap edges which are related to the Mo-d and Ru-d orbitals. By increasing temperature the well dispersed deep level bands in transport, but at low temperatures, the contribution for the transport due to low lying bands is very less and it is only from flat bands near the Fermi. The power factor is another important thermoelectric parameter ($P = S^2s$) that provides information about thermoelectric nature of materials. Fig. 8(c) has been shown the zero amount of P in the 50K to 200K interval and reached to its maximum at 600K. So this compound can be a good candidate for power generators. Finally, we calculated the dimensionless coefficients of ZT in Fig. 8(e) that is 0.98 amount in 50K and decreased gently by increasing temperature, and in the room temperature has 0.8, which indicated that this composition is a suitable case for thermoelectric application in the room temperature and lower than it. The ZT is directly related to the S, s, T and inversely to K parameters ($ZT = S^2sT/K$) and a proper thermoelectric material must have a merit coefficient of one or more.

4. Conclusions

The electronic, optical and thermoelectric calculations of the $MoRuS_2$ nano-sheet have been done based on the DFT framework with GGA approximation. Replacing the Ru atom to the Mo site in the MoS_2 nano-sheet has been changed the electronic properties of the p-type semiconductor to the n-type one by a direct energy gap by 1.8 eV amount. The total DOS diagrams in the up and down spins were referred to the non-magnetic behavior. The optical coefficient parameters were shown the semiconducting treatment along with the *xx* and *zz* light directions. Also, the energy loss functions of the light were located in the higher energies and the plasmonic oscillations occurred in these energies. So, the $MoRuS_2$ nano-sheet has the good sensitive in the IR, visible and UV edge and the light is transparent in this compound in the higher energies, completely.

Our thermoelectric results were shown that this composition has the great of power factor in the 600K, which made it for power generator applications. Also, this compound has a good ZT parameter in the 100K range around 0.98 and also, in the room temperature, around the 0.85 amount.

REFERENCES

[1] K.S. Novoselov et al., Nature **438**, 197-200 (2005).
[2] F. Ma et al., Nano Lett. **16**, 3022-3028 (2016).
[3] A. Boochani, B. Nowrozi, J. Khodadadi, S. Solaymani, S. Jalali-Asadabadi, J. Phys. Chem. C. **121** (7), 3978-3986 (2017).
[4] B.S. Mohrdarghaemmaghami, A. Boochani, S.M. Elahi, H. Khosravi, Results Phys. **8**, 1209-1215 (2018).
[5] V.L. Le, T.J. Kim, H.G. Park, H.T. Nguyen, X.A. Nguyen, Y.D. Kim, Curr. Appl. Phys. **19** (2), 182-187 (2019).
[6] Juntong Zhu et al., J. Am. Chem. Soc. **141** (13), 5392-5401 (2019).

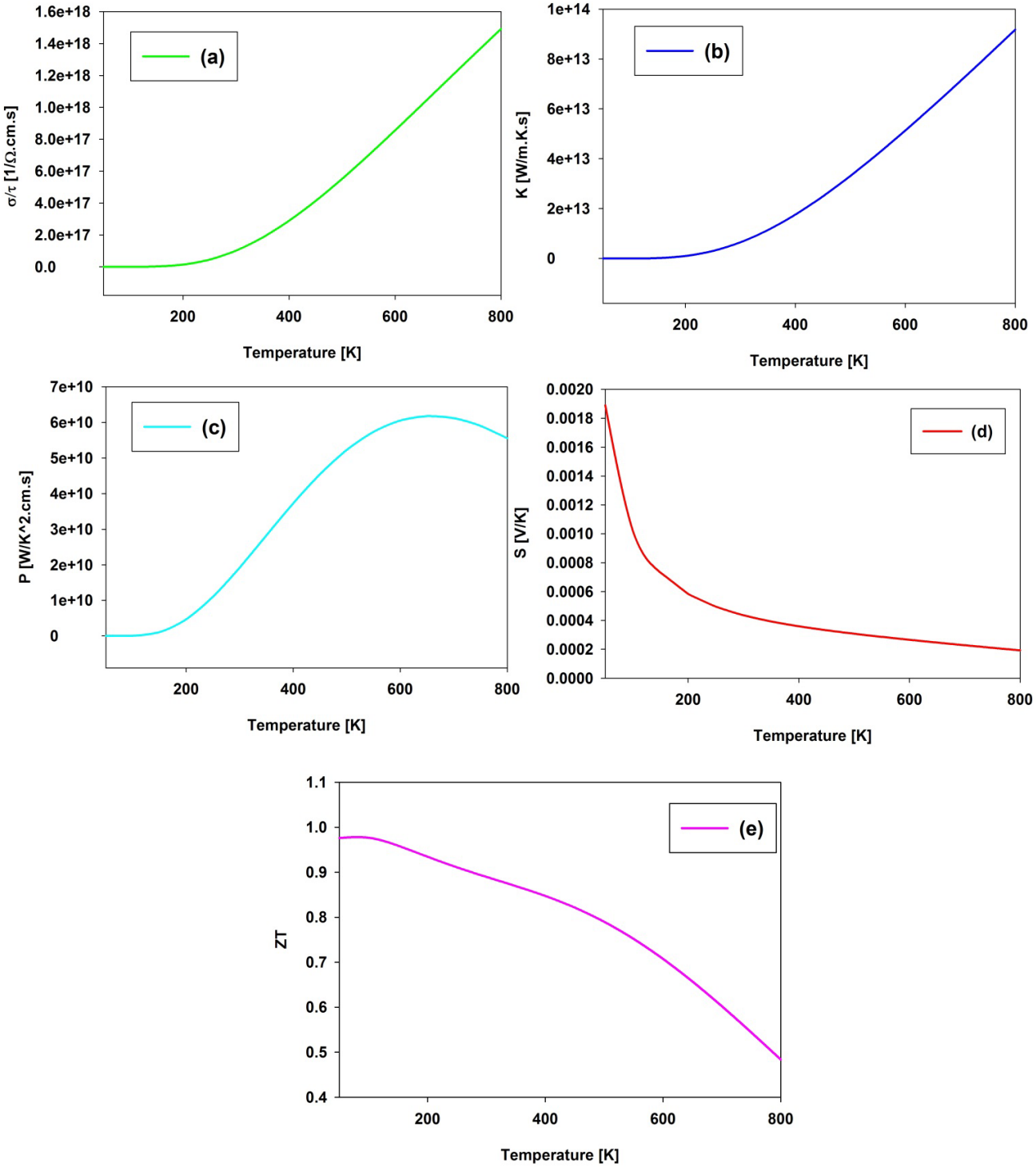

Fig. 8. The electronic conductivity, thermal conductivity, power factor, seebeck and merit coefficients versus temperature in (a-e) panels, respectively

[7] K. Sarvazad, M. Elahi, F. Ahmadian, A. Boochani, Mater. Res. Express. **6** (7), 075029-075039 (2019).

[8] M. Xu, T. Liang, M. Shi, H. Chen, Chem. Rev. **113**, 3766-3798 (2013).

[9] F.K. Perkins, A.L. Friedman, E. Cobas, P.M. Campbell, G.G. Jernigan, B.T. Jonker, Nano Lett. **13**, 668-673 (2013).

[10] H.S. Lee, S.-W. Min, Y.-G. Chang, M.K. Park, T. Nam, H. Kim, J.H. Kim, S. Ryu, S. Im, Nano Lett. **12**, 3695-3700 (2012).

[11] N. Perea-López, A.L. Elías, A. Berkdemir, A. Castro-Beltran, H.R. Gutiérrez, S. Feng, R. Lv, T. Hayashi, F. López-Urías, S. Ghosh, B. Muchharla, S. Talapatra, H. Terrones, M. Terrones, Adv. Funct. Mater. **23**, 5511-5517 (2013).

[12] B. Radisavljevic, A. Radenovic, J. Brivio, I.V. Giacometti, A. Kis, Nat. Nanotechnol. **6**, 147-50 (2011).

[13] J.N. Coleman, M. Lotya, A. O'Neill, S.D. Bergin, P.J. King, U. Khan, K. Young, A. Gaucher, S. De, R.J. Smith, Science **331**, 568-571 (2011).

[14] H. Schmidt, S. Wang, L. Chu, M. Toh, R. Kumar, W. Zhao, A. Castro Neto, J. Martin, S. Adam, B.Özyilmaz, Nano Lett. **14**, 1909-1913 (2014).

[15] Y.H. Lee, X.Q. Zhang, W. Zhang, M.T. Chang, C.T. Lin, K.D. Chang, Y.C. Yu, J.T.W. Wang, C.S. Chang, L.J. Li, Adv. Mater. **24**, 2320 (2012).
[16] Q. Feng, Y. Zhu, J. Hong, M. Zhang, W. Duan, N. Mao, J. Wu, H. Xu, F. Dong, F. Lin, Adv. Mater. **26**, 2648-2653 (2014).
[17] X. Zhao, C. Xia, T. Wang et al., J. Alloys Compd. **649**, 357-361 (2015).
[18] W.J. Yu, Z. Li, H. Zhou et al., Nat. Mater. **12**, 246-252 (2013).
[19] J. Lin, J. Zhong, S. Zhong et al., Appl. Phys. Lett. **103** (6), 063109-063113 (2013).
[20] J. Pu, Y. Yomogida, K. K. Liu et al., Nano Lett. **12**, 4013-4017 (2012).
[21] O. Lopez-Sanchez et al., Nature Nanotech. **8,** 497-501 (2013).
[22] S. Wi, H. Kim, M. Chen, H. Nam, L.J. Guo, E. Meyhofer, X. Liang, ACS Nano. **8**, 5270-5281 (2014).
[23] S. Ding, D. Zhang, J.S. Chen , X.W. (David) Lou, Nanoscale. **4**, 95-98 (2012).
[24] Y. Li, H. Wang, L. Xie, Y. Liang, G.G Hong, H. Dai, J. Am. Chem. Soc. **133**, 7296-7299 (2011).
[25] J.W. Jiang, Front. Phys. **10**, 287-302 (2015).
[26] H. Shi, H. Pan, Y.W. Zhang et al., Phys. Rev. B. **87** 155304-155312 (2013).
[27] T. M. Lei, S. B. Wu et al., Rare Metal Materials and Engineering **42**, 2477-2480 (2013).
[28] E. Gourmelon et al., Sol. Energy Mater. Sol. Cells. **46**, 115-121 (1997).
[29] M. Thomalla, H. Tributsch, J. Phys. Chem. B. **110**, 12167-12171 (2006).
[30] Ştefan Ţălu et al., Electron. Mater. Lett. **12** (5), 580-588 (2016).
[31] Arash Boochani et al., Commun. Theor. Phys. **63** (5), 641-651 (2015).
[32] Ştefan Ţălu, Miroslaw Bramowicz, Slawomir Kulesza, Shahram Solaymani, Mater. Sci. Semicond. Process **79**, 144-152 (2018).
[33] S. Majidi et al., Results Phys. **7**, 3209-3215 (2017).
[34] M. Zare et al., Sci. Rep. **8** (1), 10870-10881 (2018).
[35] M. Buscema, M. Barkelid, V. Zwiller, H.S. van der Zant, G.A. Steele, A. Castellanos-Gomez, Nano Lett. **13**, 358-363 (2013).
[36] J. Xie, H. Zhang, S. Li, R. Wang, X. Sun, M. Zhou, J. Zhou, X.W.D. Lou, Y. Xie, Adv. Mater. **25**, 5807-5013 (2013).
[37] X. Liu, G. Zhang, Q.-X. Pei, Y.-W. Zhang. Appl. Phys. Lett. **103**, 133113-133121 (2013).
[38] Y. Cai, J. Lan, G. Zhang, Y.-W. Zhang, Phys. Rev. B. **89**, 035438-035446 (2014).
[39] R. Yan, J.R. Simpson, S. Bertolazzi, J. Brivio, M. Watson, X. Wu, A. Kis, T. Luo, A.R. Hight Walker, H.G. Xing, ACS Nano. **8**, 986-993 (2014).
[40] Z. Jin, Q. Liao, H. Fang, Z. Liu, W. Liu, Z. Ding, T. Luo, N. Yang, Sci Rep. **5**, 18342-18349 (2015).
[41] K. Hippalgaonkar, Y. Wang, Y. Ye, D.Y. Qiu, H. Zhu, Y. Wang, J. Moore, S.G. Louie, X. Zhang, Phys. Rev. B. **95**, 115407-115413 (2017).
[42] H. Babaei, J.M. Khodadadi, S. Sinha, Appl. Phys. Lett. **105**, 193901-193907 (2014).
[43] W. Huang, X. Luo, C.K. Gan, S.Y. Quek, G.C. Liang, Phys. Chem. Chem. Phys. **16**, 10866 -10874 (2014).
[44] S. Bhattacharyya, T. Pandey, A.K. Singh, Nanotechnology. **25** (46), 465701-465714 (2014).
[45] Yu Cai, Xi Yang, Tao Liang, Lu Dai, Lin Ma, Guowei Huang, Weixiang Chen, Hongzheng Chen, Huanxing Su, Mingsheng Xu, Nanotechnology **25** (46), 465401-465407 (2014).
[46] P. Blaha, K. Schwarz, P. Sorantin, S.B. Trickey, Comput. Phys. Commun. **59**, 399-415 (1990).
[47] P. Blaha, K. Schwarz, G.K.H. Madesen, D. Kvasnicka, J, Luitz, WIEN2K, An Augmented Plane Wave + Local Orbitals Program for Calculating Crystal Proper-ties, Karlheinz Schwarz, Techn; Universitaetwien:Wein, Austria, 2001.
[48] J. Perdew, J.A. Chevary, S.H. Vosko, K.A. Jackson, M.R. Pederson, D.J. Singh, C. Fiolhais, Phys. Rev. B. **46**, 6671-6678 (1992).
[49] H.J. Monkhorst, J.D. Pack. Phys. Rev. B. **13**, 5188-5195 (1976).
[50] R.L. Kronig, J. Opt. Soc. Am. **12**, 547-557 (1926).
[51] G.K.H. Madsen, D.J. Singh, Comput. Phys. Commun. **175**, 67-71 (2006).
[52] A.M. Fox, Optical Properties of Solids. Oxford University Press, (London 2001).
[53] F. Wooten, Optical Properties of Solids. Academic Press, New York and (London 1972).
[54] W. Liang, A.I. Hochbaum, M. Fardy, O. Rabin, M. Zhang, P. Yang, Nano Lett. **9**, 1689-1693 (2009).
[55] K. Biswas, J. He, I.D. Blum, C.-I. Wu, T.P. Hogan, D.N. Seidman, V.P. Dravid, M.G. Kantazidis, Nature **489**, 414-418 (2012).
[56] G.J. Snyder, E.S. Toberer, Nat. Mater. **7**, 105-114 (2008).